

Contents lists available at ScienceDirect

Heliyon

journal homepage: www.cell.com/heliyon



Research article



Fault diagnosis of accelerometer servo circuit output saturation based on feature electrical parameters extraction

Ming Zhang^{*}, Xin Xu, Likun Xu, Xiaoming Ruan, Duan Zhou, Zhenshan He

Xi'an Microelectronics Technology Institute, 26 Information Avenue, Chang'an District, Xi'an, China

ARTICLE INFO

Keywords: Microelectronic device Servo circuit of quartz flexible accelerometer Output saturation Feature electrical parameters extraction Fault diagnosis Hybrid integrated Improvement measures

ABSTRACT

The servo circuit of quartz flexible accelerometer is an extremely vital microelectronic device in inertial system. The paper introduces the traditional analysis process about output saturation fault of accelerometer servo circuit. For the shortcomings of traditional analysis methods, a fault diagnosis method based on feature electrical parameters extraction is proposed. According to the fault phenomenon, combined with the modular characteristics of hybrid integrated circuits, the feature electrical parameters of fault modes are extracted, and the fault modes' judgment basis is set. By the judgment results of the feature electrical parameters of the fault circuit, the circuit with output saturation fault caused by the electrical damage to the differential capacitance detector and other faults can be located quickly and accurately, and it is verified by the analysis of faulty circuit samples. Targeted for these faults, the improvement measures are put forward. This analysis method improves the fault diagnosis efficiency and reliability about the accelerometer servo circuit, and has guiding significance for enhancing the success rate of the failure analysis in the hybrid integrated circuits.

1. Introduction

Quartz flexible accelerometer is an emblematic class of torque balanced pendulum accelerometer which integrates the flexible supporting part with the capacitive sensor and has the function of signal conversion. It has the advantages of excellent sensitivity, high accuracy, well reliability and good stability, so it has been widely used in national strategic fields and civil emerging industries such as aerospace flight control, precision guidance of long-range weapons, microgravity measurement, railway track inspection, vehicle body vibration monitoring, and inclinometer system while drilling for oil and mineral resources [1–5]. As a signal conversion module, the servo circuit monitors the change of the differential capacitance of the accelerometer sensor, transforms it into a direct current signal, and then completes the operation of the acceleration of the motion carrier and the required physical quantity [6]. With the continuous expansion of the application field of the servo circuit, the requirement for it is becoming higher, and the application environment is becoming more complex. Although the complete screening tests can effectively eliminate the early failure of the circuit, various fault phenomena occur from time to time, mainly including no output, output oscillation, output saturation, and parameter drift. These faults will result in abnormality of system output and even functional failure in severe cases [7–9]. In view of various failure modes mentioned above, it is necessary to implement fault analysis, and the first step of it is to locate the fault fast and determine the fault mode.

E-mail address: zhangm_work@163.com (M. Zhang).

^{*} Corresponding author.

During the large-scale and high-yield saturated production of hybrid integrated circuits, the traditional fault analysis methods have more and more shortcomings such as complex process, long time and low success rate. With the development of fault analysis technology, the fast fault diagnosis method has become a hot spot on fault analysis and reliability research of hybrid integrated circuits [10-12]. The fault dictionary detection method can accurately locate the fault of electronic components accurately, but for the multi-level complex hybrid integrated circuits, the actual fault detection process has a large workload [13–17]. Using machine learning fault diagnosis method can realize fault mode recognition quickly, but it needs a lot of fault data for fast learning and training [18–20]. The fault diagnosis method based on feature selection and extraction can be efficiently applied to the fault diagnosis method of analog circuits [21,22]. Model-based fault diagnosis methods can be extensively used in various industrial fields [23-29]. Besides, the fault diagnosis is based on the good integrity of the faulty circuit sample analysis process without introducing the external damage, mechanical damage or other factors that cause the failure analysis to stop. Due to the limitation of manufacturing technology and traditional fault analysis method of the accelerometer servo circuit, the circuit is likely to be damaged in the analysis process, which affects the reliability of the fault analysis seriously. In this paper, a fault diagnosis method using feature electrical parameters extraction is proposed, which can quickly and accurately analyze the circuit output saturation failure caused by the electrical damage to the differential capacitance detector. At the same time, it can be extended to other failure modes of output saturation. The application of this method is of great significance for distinguishing the failure modes and promoting the efficiency and reliability of failure analysis.

2. The traditional fault analysis on accelerometer servo circuit with output saturation

The servo circuit matching the sensor is a typical product using hybrid integrated manufacturing technology. During its the long-term development and production process, the failure analysis engineers have accumulated rich failure analysis experience and formed a failure analysis program for the circuit. In general, the common methods for failure analysis of the circuit include external visual inspection, X-ray inspection, I–V characteristic curve analysis, electrical performance test, internal visual inspection, conduction band on-off test, non-destructive tensile test, key fault nodes test, scanning optical inspection, energy spectrum analysis, component replacement test, and destructive physical analysis. For the output saturation fault of accelerometer servo circuit, the traditional analysis method is to confirm the destructive mechanical damage by external visual inspection firstly. Then the internal gold bonding wire and capacitors are checked by X-ray inspection. Subsequently, the input and output port characteristics of fault circuit are preliminarily analyzed using the transistor characteristic plotter. After the above inspection, the saturation fault phenomenon can be confirmed by electrical performance test. It can be seen that the electrical performance test is extremely important for judging the failure phenomenon about output saturation. In order to find further failure cause, the failure circuit has to be mechanically uncapped. After opening the cap, the physical inspection is performed, such as internal visual inspection and conduction band on-off test, and

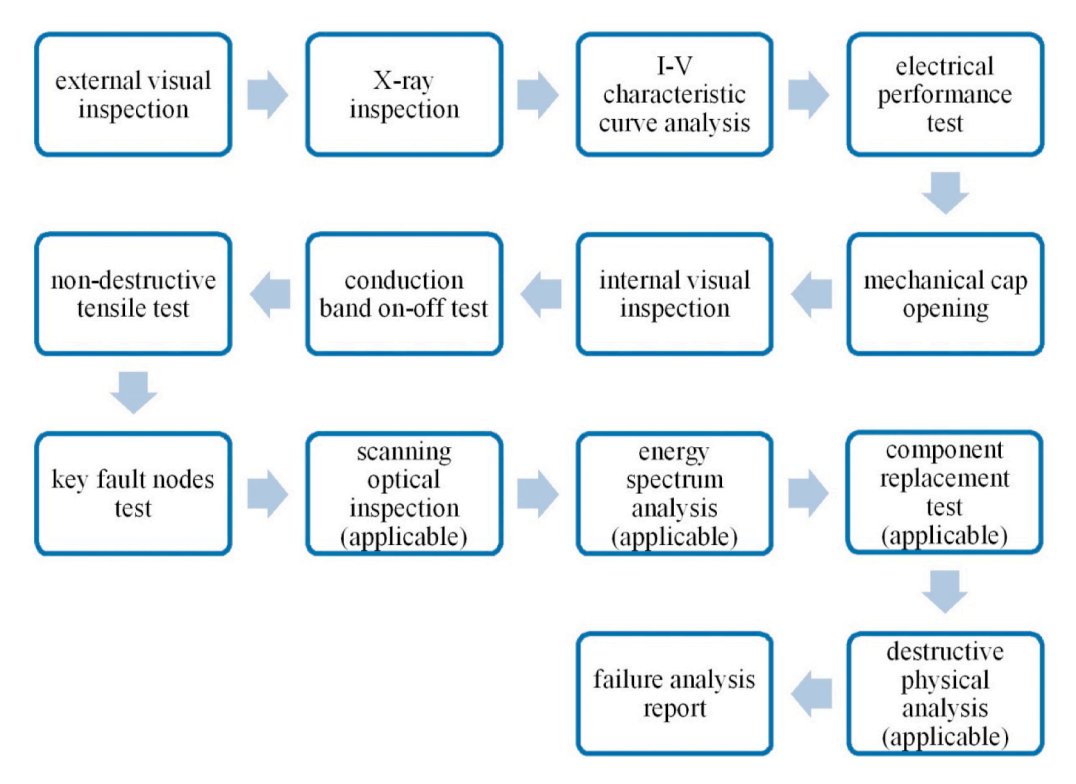


Fig. 1. The flow chart of traditional failure analysis on the accelerometer servo circuit.

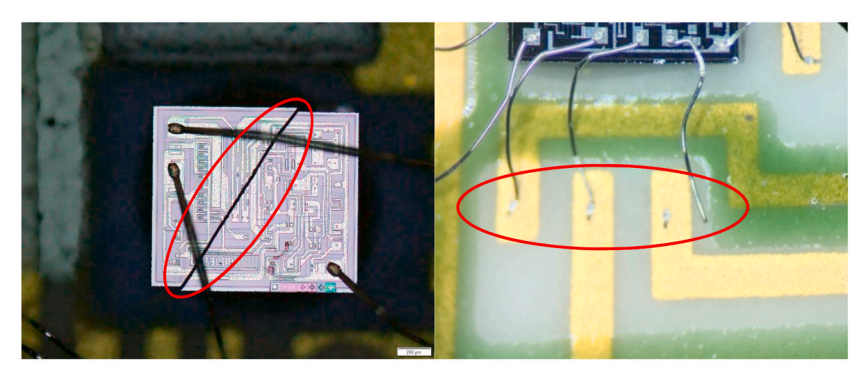
then non-destructive tensile test is conducted. If no abnormality is found during the above inspection, it is necessary to conduct electrical test on the key fault nodes of the circuit to preliminarily locate the fault location. The judged fault location is further checked with fault analysis equipment, such as scanning optical inspection and energy spectrum analysis. Finally, the fault location is confirmed by component replacement test, the fault cause and mechanism are analyzed, and the failure analysis report is formed [8,9]. The flow chart of traditional failure analysis on the servo circuit is shown in Fig. 1.

Obviously, the traditional fault analysis method is a fault analysis for all fault modes of the accelerometer servo circuit, but it is difficult to perform targeted analysis for various types of output saturation faults. This analysis method still mainly relies on physical analysis, with complex steps, many instruments and equipment involved, long time and heavy workload. Wan et al. [8] and Zhang et al. [9] successfully completed the task using traditional fault analysis methods, but the workload was also enormous. Starzyk et al. [17] proposed an effective method for selecting the optimal test point set for dictionary technology in simulated fault diagnosis. Its main feature is to search for the local optimal test point set, but there has been little research on subsequent fault analysis.

The servo circuit matching the sensor for mass production is a hybrid integrated circuit based on a metal shell with a semicircular ceramic cap, which is sealed with insulating epoxy adhesive. During mechanical cap opening, analysis of internal components and component replacement test, it is possible to cause damage to faulty circuit samples, such as chip fracture, bonding wire damage, capacitance damage, and substrate crack, as shown in Fig. 2 (a) \sim 2 (d). These damages will affect the subsequent failure analysis, and may lead to the termination of failure analysis in serious cases. He et al. [19] and Aminian et al. [20] focused on the discussion of fast diagnostic analysis methods, and there is relatively little research on the reliability of analysis. For the sake of improving the reliability and efficiency of fault analysis, a fault diagnosis method based on feature electrical parameters extraction is proposed.

3. Fault diagnosis method based on feature parameters extraction

According to the fault phenomenon of the accelerometer servo circuit, combined with the modular characteristic of the hybrid integrated circuit, the fault diagnosis method based on feature electrical parameters extraction is studied. Firstly, the feature electrical parameters of accelerometer servo circuit fault mode are extracted. Secondly, the criteria of fault feature electrical parameters are set to judge the fault mode of the accelerometer servo circuit. Finally, on the basis of the judgment results of the feature parameters, targeted physical analysis and verification are performed to complete the fault diagnosis.



(a) Chip fracture

(b) Bonding wire damage



(c) Capacitance damage

(d) Substrate crack

Fig. 2. Faulty circuit sample damage.

3.1. Extraction of fault feature electrical parameters

The purpose of the extraction of feature electrical parameters is to find out the functional parameters used to distinguish the fault circuit from the non-fault circuit or other faults for a specific fault mode of the circuit. According to the electrical characteristics of faulty circuit samples, accurate positioning can be provided for subsequent physical fault diagnosis. As a matter of course, this paper will take the most common output saturation failure mode of quartz flexible accelerometer as a case for analysis. After completing the cross-interchange test, visual inspection, I–V characteristic test and electrical performance test, the fault mode caused by the explicit fault factors is eliminated on the basis of the failure phenomenon and electrical performance parameters. Then, the fault feature electrical parameters are extracted based on the principle of accelerometer servo circuit for the further analysis. The principle diagram of accelerometer servo circuit is shown in Fig. 3.

The servo circuit is basically made up of a positive voltage regulator, a negative voltage regulator, a differential capacitance-voltage converter, a transconductance/compensation amplifier and related resistors and capacitors. Accelerometer servo circuit output saturation fault means that in the acceleration range measurement range, the circuit output voltage does not change with the change of acceleration, and has fixed output circuit maximum voltage. This fault is a common fault of accelerometer servo circuit, which belongs to a functional fault. In the field of inertial navigation, it is well known that 0 g refers to an equilibrium state with acceleration of 0. At this time, the pendulum in the differential capacitance sensor is in the middle of the two pole plate position. In the case of absolute 0 g, the pendulum quartz reed is neither subjected to the inertial force of acceleration nor the ampere force, so the circuit output voltage is 0 V. It can be seen that the output voltage of the 0 g state is an important parameter for accelerometer servo circuit fault detection. As both the voltage regulators are tested normally in the electrical performance test, it is logical to check the differential capacitancevoltage converter. The pin7 and pin8 are the input ports of the circuit, which is only used to connect the differential capacitance signals generated by quartz pendulum of the sensor. When the accelerometer sensor is in the 0 g state, the capacitance values of differential capacitor1 and differential capacitor2 in the differential capacitance sensor are equal. When a triangle wave with fixed frequency and amplitude is produced by the reference triangle wave generator on the base of the transistors connected to the differential capacitor detector, if the transistors are periodically turned on and off, the differential capacitor1 and differential capacitor2 in the differential capacitance detector generate periodic trapezoidal wave signals. Because the carrier signals connected to pin7 and pin8 of the circuit are provided by the same reference triangular wave signal, the amplitude of the trapezoidal wave signal detected by these two pins in the normal circuit in the 0 g state should be the same. Therefore, the signals of these two pins of the faulty circuit with load are detected by oscilloscope. It is found that the pin7 has no signal, and the pin8 is a trapezoidal wave signal with the amplitude of 3.36 V. Further, after removing the accelerometer sensor, the test without load is carried out. It is found that the pin7 is a trapezoidal wave signal with the amplitude of 0.79 V, and the pin8 is a trapezoidal wave signal with the amplitude of 3.71 V. In fact, these two pins of the qualified circuit are trapezoidal waves with the same amplitudes about 3.3 V with load, and their amplitudes are about 4.0 V without load. There is a difference between the detection waveform of the faulty circuit and that of the pin7 of the qualified circuit, that is, the trapezoidal amplitude of pin7 of the faulty circuit is smaller than that of pin8. See Table 1 for the detection waveforms. The above detection shows that the differential capacitance detector is abnormal.

The carrier wave of the differential capacitance detector is created by the reference triangle wave generator, so it is logical to detect the reference triangle wave generator. The reference triangular wave amplitude of the faulty circuit is 4.98 V, as shown in Fig. 4 (a), and the qualified circuit is shown in Fig. 4 (b). This indicates that the reference triangle wave generator is normal.

It is reasonable to check the subsequent module of abnormal position. By the voltage self-test detection, it is found that the positive saturation output voltage (V_{sat1}) and negative saturation output voltage (V_{sat2}) of the faulty circuit are good. See Table 2 for the test data. The test results show that the preamplifier and transconductance/compensation amplifier can work normally and the electrical

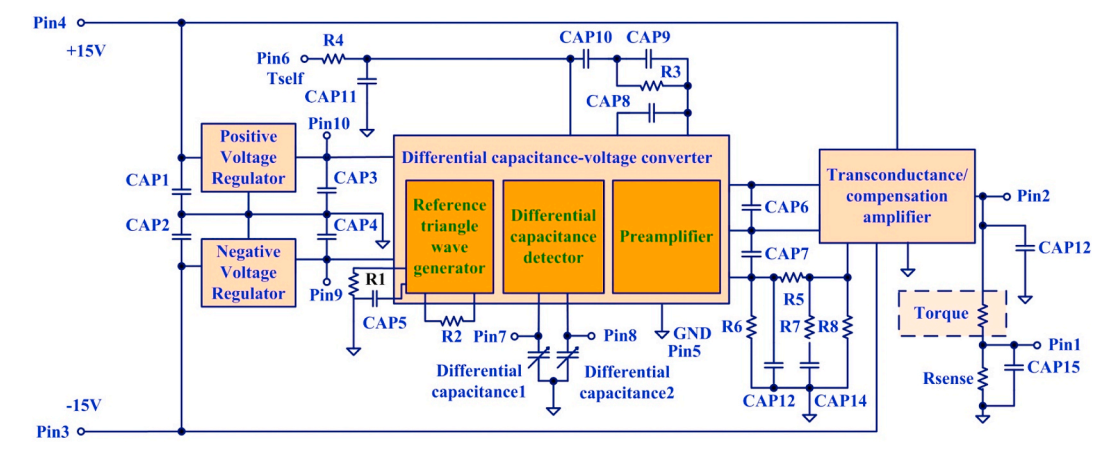
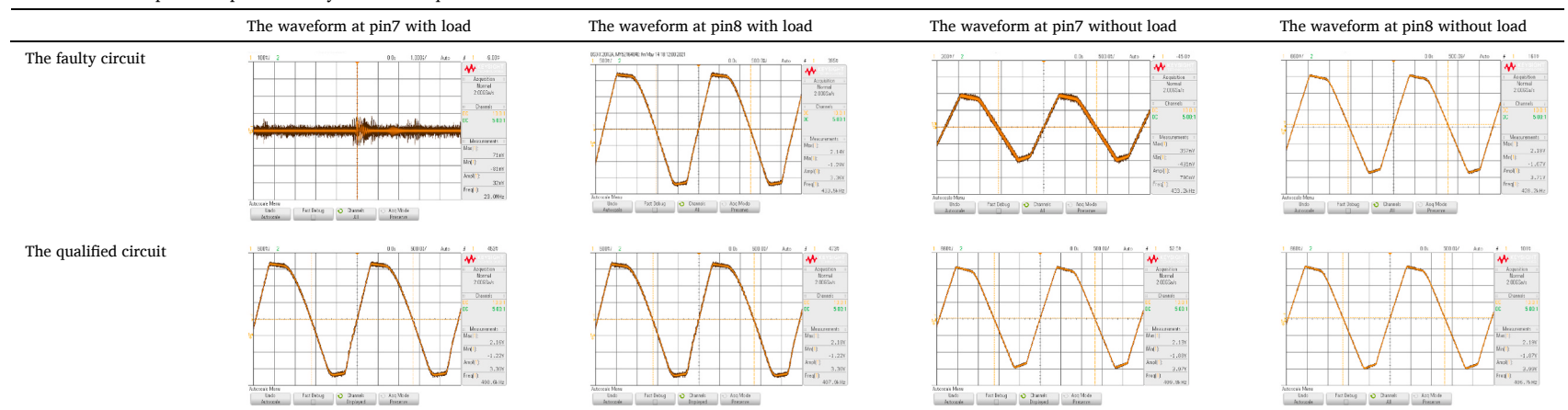


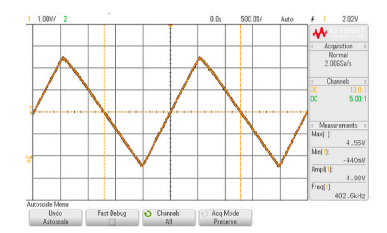
Fig. 3. Principle diagram of accelerometer servo circuit.

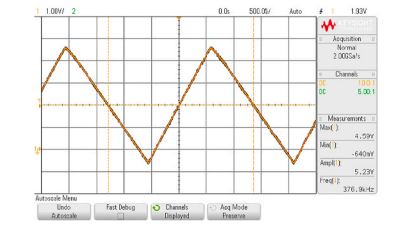
Heliyon 10 (2024) e28382

 Table 1

 The waveforms at pin7 and pin8 of faulty circuit and qualified circuit.







(a) The waveform of the faulty circuit

(b) The waveform of the qualified circuit

Fig. 4. The waveforms of reference triangle wave generator.

Table 2The voltage self-test results of the faulty circuit and the qualified circuit.

	V _{sat1} (V)	V _{sat2} (V)
The faulty circuit	11.22	-11.94
The qualified circuit	11.25	-11.99
Range of typical values for qualified circuit	10~13	-13 ~ -11

Table 3The diode characteristic voltages from pin7 to pin8 and pin8 to pin7.

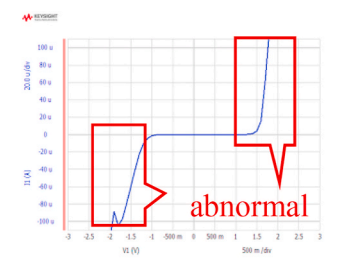
	V_{T1}	V_{T2}
The faulty circuit	1.61	2.18
The qualified circuit	1.40	1.40

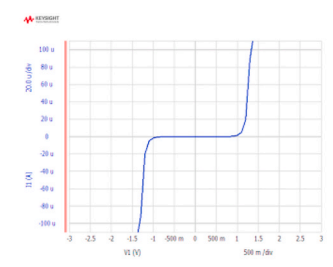
parameters are normal.

From the above detection, it is initially considered that the fault is in the differential capacitance detector. The diode characteristic voltage tests using digital voltmeter shows that the voltage from pin7 to pin8 (V_{T1}) is 1.61 V, while the diode characteristic voltage from pin8 to pin7 (V_{T2}) is 2.18 V. However, the diode characteristic voltage of pin7 to pin8 and pin8 to pin7 should be about 1.40 V in accordance with the circuit principle analysis and actual test, as shown in Table 3.

It can be seen from the above test that the diode characteristic voltages between these two pins of the faulty circuit are abnormal. As a supplementary experiment, the I–V characteristic curve between these two pins of the faulty circuit is tested, and it is found that the test results are abnormal, as shown in Fig. 5(a). The curve of the qualified circuit is shown in Fig. 5 (b). The circuit failure is related to the abnormal electrical characteristics between pad13 and pad14 of the internal converter component, because the pad13 is connected to pin7 and the pad14 is connected to pin8. All in all, the above test results are corresponded to the fault mode caused by electrical damage to the differential capacitance detector.

For the circuit with output saturation failure mode caused by the above condition, the electrical parameters that need to be paid attention to include the output voltage in the state of 0 g, the positive power supply static current, the negative power supply static current, the self-test positive saturation output voltage, the self-test negative saturation output voltage, the waveform and amplitude of the reference triangle wave generator, the waveforms detected at pin7 and pin8 of the circuit with load, the waveforms detected at these two pins of the circuit without load, the diode characteristic voltage from pin7 to pin8 of the circuit, and the diode characteristic voltage from pin8 to pin7 of the circuit. These parameters are extracted and taken as the feature parameters group of this failure mode.





(a) The pin7 to pin8 of the faulty circuit

(b) The pin7 to pin8 of the qualified circuit

Fig. 5. The I-V characteristic curve test.

3.2. Setting of fault feature electrical parameters

The above mentioned feature electrical parameters are set in grades:

(1) The output voltage in the state of 0 g (V_{0g}), the positive static current (I_{cc}) and the negative static current (I_{ee}) are first-level decision feature parameters, which are marked as a1, a2 and a3. If the V_{0g} is from 10 to 13 V, set a1 to 1, or set a1 to 0. If I_{cc} ranges from 30 to 39 mA, set a2 to 1, otherwise, set a2 to 0. If I_{ee} ranges from 6.5 mA to 10 mA, a3 is set to 1, or a3 is set to 0. This stage of decision feature parameters can determine whether the fault phenomenon is output saturation or not.

- (2) The self-test positive saturation output voltage (V_{sat1}) and self-test negative saturation output voltage (V_{sat2}) are second-level decision feature parameters, which are marked as b1 and b2. If the positive saturation output voltage of the self-test is 10–13 V, set b1 to 1. Otherwise, set it to 0. If the negative saturation output voltage is -13 to -10 V, set b2 to 1. Otherwise, set b2 to 0. This stage decision feature parameters can determine whether the preamplifier of the converter or the transconductance/compensation amplifier is abnormal, and distinguish other output saturation failure modes.
- (3) The waveform and amplitude of the reference triangle wave generator is third-level decision feature parameter, which is marked as c. If the waveform and amplitude of the reference triangle wave are normal, set it to 1. If the reference triangle wave has no waveform, abnormal waveform, or abnormal parameter, it is set to 0. This stage decision feature parameters can judge whether the reference triangle wave generator of differential-capacitance voltage converter is faulty or not and distinguish other output saturation failure modes.
- (4) The waveforms detected at pin7 and pin8 of the circuit with load, the waveforms detected at these two pins of the circuit without load, the diode characteristic voltage (V_{T1}) from pin7 to pin8 and the diode characteristic voltage (V_{T2}) from pin8 to pin7 are fourth-level decision feature parameters, and the four parameters above are marked as d1, d2, d3 and d4. Firstly, if waveforms detected at either pin7 or pin8 with load are abnormal, d1 is set to 1. If the waveforms detected at pin7 and pin8 with load are the same and normal, d1 is set to 0. Secondly, if the waveforms detected either at pin7 or pin 8 without load are abnormal, d2 is set to 1. If the waveforms detected at pin7 and pin8 without load are the same and normal, d2 is set to 0. Thirdly, if the V_{T1} is abnormal but not open circuit or short circuit, d3 is set to 1. Otherwise the d3 is set to 0. Lastly, if the V_{T2} is abnormal but not open circuit or short circuit, the d4 is set to 1. Otherwise the d4 is set to 0. This stage decision feature parameters can judge whether the differential capacitance detector of differential capacitance-voltage converter is faulty or not, and distinguish other output saturation failure modes.

From the above settings, the discriminant about the feature parameters of the output saturation failure mode caused by the above condition is obtained, which is expressed as equation (1).

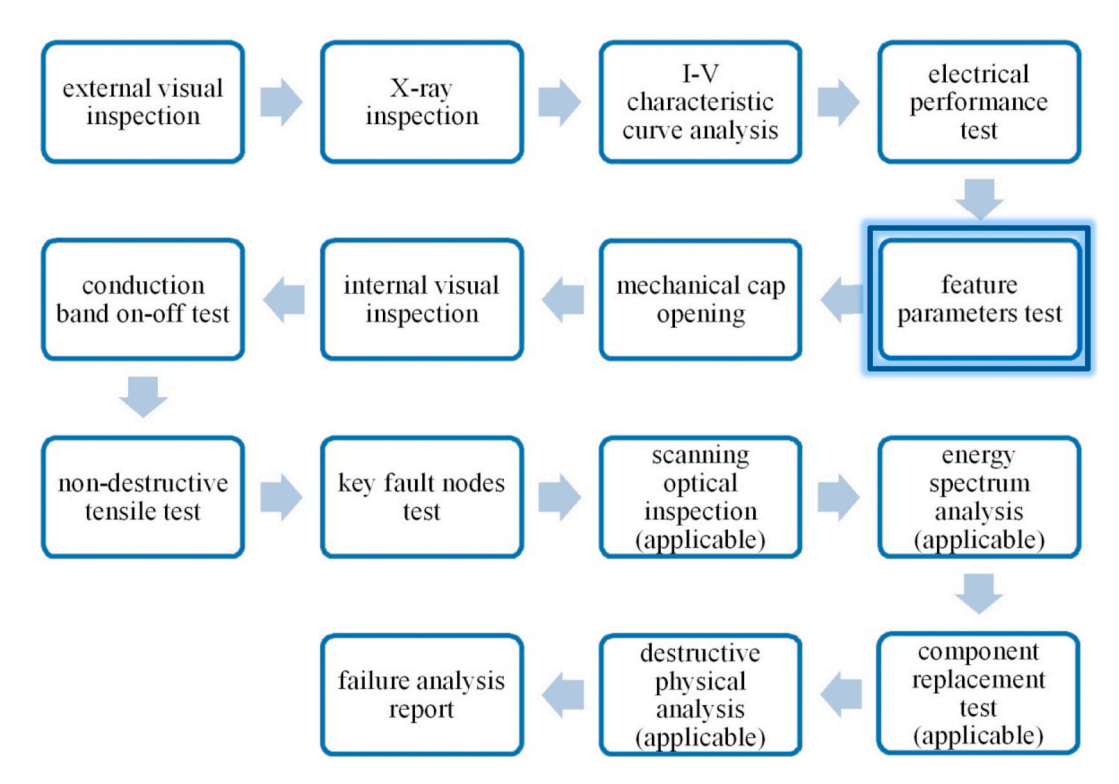
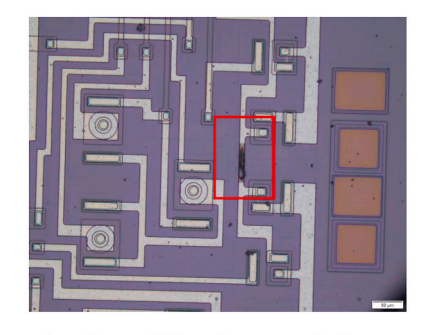
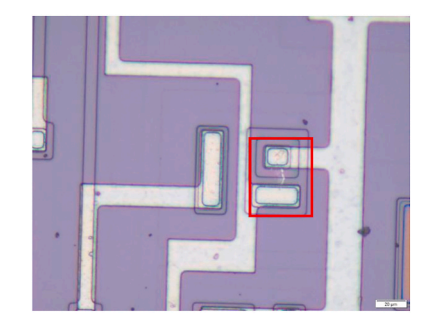


Fig. 6. The flow chart of the fault analysis using feature parameters extraction.





(a) Burnt local amplification morphology

(b) Diode breakdown amplification morphology

Fig. 7. Morphology of the faulty circuit with metallographic microscope.

$$F(a1,a2,a3,b1,b2,b3,c,d1,d2,d3,d4) = (a1 \& a2 \& a3) \& (b1 \& b2 \& b3) \& (c) \& (d1 \& d2 \& d3 \& d4)$$
(1)

If F(a1, a2, a3, b1, b2, b3, c, d1, d2, d3, d4) = 1, the failure mode is mentioned in this section, and if F(a1, a2, a3, b1, b2, b3, c, d1, d2, d3, d4) = 0, the failure mode is not this.

3.3. Specific physical analysis verification

When the feature electrical parameters of the fault circuit are set and the feature parameters meet the result of the feature parameter discriminant of a certain failure mode, the fault localization can be completed, the failure mode can be predicted, and targeted physical analysis and verification can be carried out quickly after the circuit is uncapped. Because the feature parameters test of the failure circuit is preceded by the open cap analysis, the failure analysis of the faulty circuit sample will not be affected or hindered even if other modules of the faulty circuit sample are damaged during the open cap analysis. The subsequent analysis steps can be simplified according to the results of the internal visual inspection after the mechanical open cap of the faulty circuit. The flow chart of the fault analysis using feature parameters extraction is shown in Fig. 6.

The feature parameters of the faulty circuit mentioned above meet the discriminant of the feature parameters of the failure mode mentioned in this section, that is, F(a1, a2, a3, b1, b2, b3, c, d1, d2, d3, d4) = 1. After the circuit is uncapped, the related module is directly internal inspected. It is found that the aluminum bar between pin 13 and pin 14 of the differential capacitance-voltage converter is burnt, as shown in Fig. 7(a). Besides, the diode connected to the pin 13 is burnt and breakdown, as shown in Fig. 7(b). This method can quickly and accurately locate the output saturation fault mode.

4. Application of fault diagnosis method based on feature parameter extraction

The faulty circuit samples caused by output saturation during assembly, screening and use are selected for analysis. Completing the analysis before opening the cap, it is confirmed that samples1-6 are intact samples, and sample7 is locally destroyed during the accelerometer cross-interchange, which is considered as a destructive sample. In the previous section, the feature parameters of the circuit with output saturation fault caused by the electrical damage to the differential capacitance detector have been extracted. Next, the method will be used to quickly locate and analyze the fault circuit samples.

4.1. Intact sample analysis

Firstly, it is reasonable to detect the feature parameters of intact fault circuit samples. Observe Table 4 for the test data about first-level decision feature parameters. It can be seen that the six circuit samples all meet the feature parameters of output saturation fault. Secondly, the faulty circuit samples1-6 are detected by voltage self-test. See Table 5 for test data of the second-level decision feature

Table 4The test data of the first-level decision feature parameters.

	$V_{og}(V)$	I _{cc} (mA)	I _{ee} (mA)
Faulty circuit sample 1	11.23	36.7	9.3
Faulty circuit sample 2	11.24	35.8	8.7
Faulty circuit sample 3	11.27	35.7	9.0
Faulty circuit sample 4	11.23	36.1	9.3
Faulty circuit sample 5	11.29	36.3	9.1
Faulty circuit sample 6	11.29	33.5	6.9
Range of typical values	≤0.01	9.5 ~ 13	6.5 ~ 10.0

Table 5The test data of the second-level decision feature parameters.

	V _{sat1} (V)	V _{sat2} (V)
Faulty circuit sample 1	11.22	-11.94
Faulty circuit sample 2	11.25	-11.94
Faulty circuit sample 3	11.25	-11.98
Faulty circuit sample 4	11.25	-12.00
Faulty circuit sample 5	11.29	11.29
Faulty circuit sample 6	11.29	-11.96
Range of typical values	10~13	-13~-11

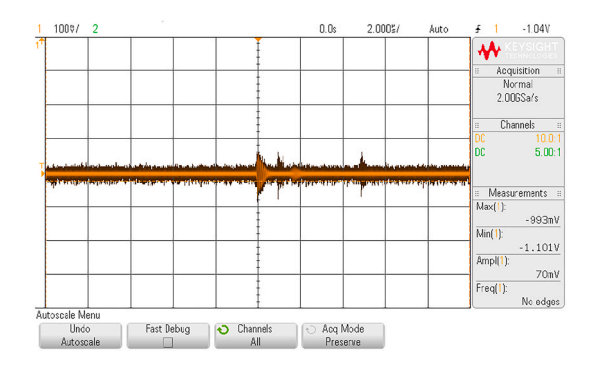


Fig. 8. Reference triangle wave of the faulty circuit sample6.

parameters. It is found that the output of the sample5 is not controlled by the self-test signal. The Vsat2 of sample5 is different from the parameters of the other fault circuit samples. It can be determined that the fault of this circuit does not belong to the output saturation mentioned in the previous section.

Thirdly, it is usual to detect the third-level decision feature parameters by oscilloscope, and it is easy to find that the fault circuit sample6 has no reference triangle wave, as shown in Fig. 8. However, the reference triangle waves of other fault circuit samples are normal. This test shows that the output saturation of the fault circuit sample6 is related to the reference triangle wave generator.

Finally, the oscilloscope is used to detect the fourth-level decision feature parameters of the faulty circuit samples. It is obvious that the waveforms with load and without load detected at pin7 or pin8 of the faulty circuit sample 1-4 are abnormal. Meanwhile, it is found that the waveforms detected at pin7 and pin8 of the faulty circuit sample5 with load are abnormal, but the waveforms detected at pin7 and pin8 without load are the same and normal. In addition, the waveforms of the fault circuit sample6 detected at pin7 and pin8 are abnormal because of no signal. The test of the fourth-level decision feature parameters about the waveforms at pin7 and pin8 are shown in Table 6.

The digital voltmeter is used to test the diode characteristic voltage of the fourth-level decision feature parameters. It is recognized that the test parameters of the fault circuit samples1-3 are abnormal, the test results of the faulty circuit sample4 is infinite, while the test results of the fault circuit sample5-6 are normal, as is presented in Table 7. It is further confirmed that the faulty modes of fault circuit samples4-6 are different from the faulty mode of fault circuit samples1-3.

The feature parameters of these faulty circuit samples are normalized. According to the fault diagnosis method using the feature parameters extraction and the discriminant results of the output saturation fault mode, it can be concluded that faulty circuit samples1-3 are output saturation fault mentioned in the previous section, and faulty circuit samples4-6 are output saturation faults caused by other reasons, as shown in Table 9 for details.

After the faulty circuit samples1-3 are uncapped, the differential capacitance-voltage converters are observed directly. It is obvious that the aluminum bar between pad13 and pad14 of the differential capacitance-voltage converters is burnt and the diodes break down, as shown in Table 10. Therefore, the fault circuit samples 1–3 are consistent with the failure mode of the fault circuit. It can be seen that the fault analysis method based on feature parameters extraction can quickly and accurately diagnose the output saturation fault of accelerometer servo circuit caused by the electrical damage to differential capacitance detector.

For fault sample 4, the feature parameters suitable for this fault mode are extracted. When performing the grades setting, the d3 and d4 in the fourth-level decision feature parameters consisting of the waveforms detected at pin7 and pin8 of the circuit with load, those without load, the diode characteristic voltage (V_{T1}) from pin7 to pin8 and the diode characteristic voltage (V_{T2}) from pin8 to pin7 are changed. If the V_{T1} is open circuit, d3 is set to 1, otherwise d3 is set to 0. If V_{T2} is open circuit, d4 is set to 1, otherwise the d4 is set to 0. The rest of the settings remain unchanged. At this point, the feature parameters of these faulty circuit samples are normalized, see Table 11.

From the above settings, the discriminant about the feature parameters of the output saturation failure mode caused by the disconnection of external lead bonding wire connecting the pin7 is obtained, which can be expressed as equation (2).

Table 6Test results of the fourth-level decision feature parameters about the waveforms at pin7 and pin8.

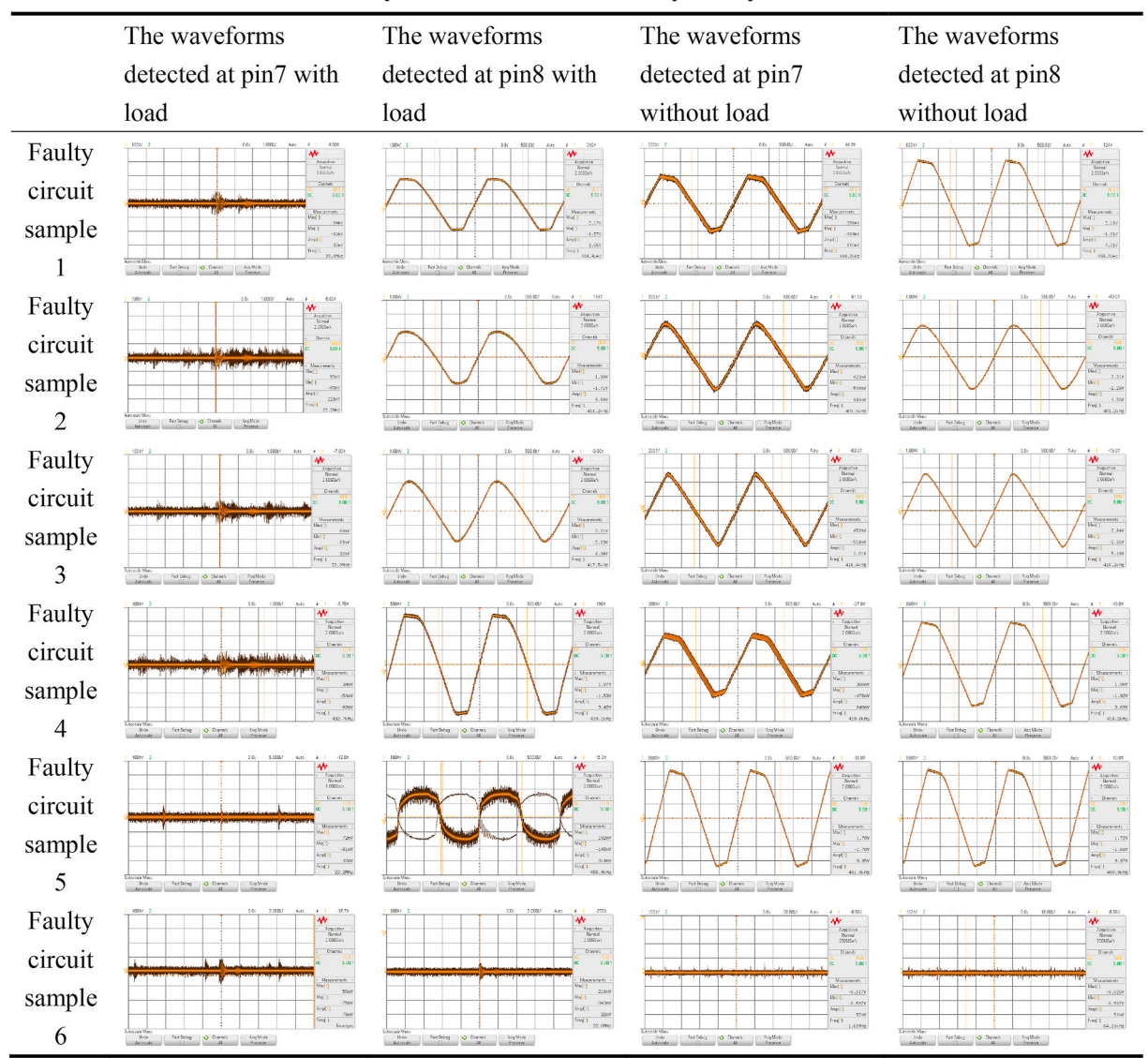


Table 7The test results of the fourth-level decision feature parameters about the diode characteristic voltage.

	the diode characteristic voltage from pin7 to pin8	the diode characteristic voltage from pin8 to pin7	Judgment result
Faulty circuit sample 1	1.66	2.22	abnormal
Faulty circuit sample 2	1.72	2.19	abnormal
Faulty circuit sample 3	1.77	1.83	abnormal
Faulty circuit sample 4	∞	∞	abnormal
Faulty circuit sample 5	1.42	1.42	normal
Faulty circuit sample 6	1.44	1.44	normal

The I–V characteristic curve between the pin7 and pin8 of the faulty circuit samples1-6 are examined by the transistor characteristic plotter, and it is observed that the characteristic curve between these two pins of the faulty circuit samples1-4 are abnormal, and the connection between these two pins of the faulty circuit sample4 is open circuit, as shown in Table 8.

 Table 8

 The I–V characteristic curve between the pin7 and pin8.

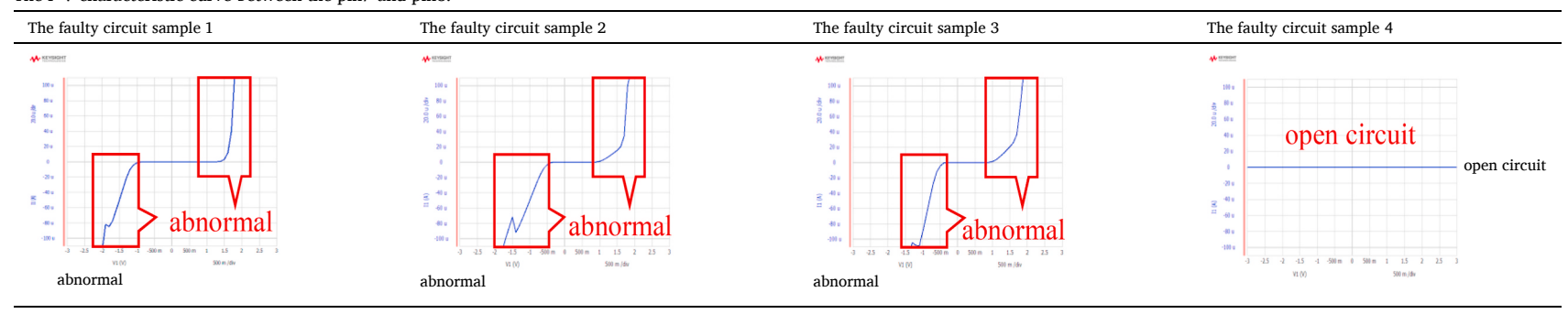


Table 9
The feature parameters function Table 1 of output saturation fault mode for fault circuit samples1-6.

	a1	a2	аЗ	b1	b2	с	d1	d2	d3	d4	result
F1	1	1	1	1	1	1	1	1	1	1	1
F2	1	1	1	1	1	1	1	1	1	1	1
F3	1	1	1	1	1	1	1	1	1	1	1
F4	1	1	1	1	1	1	1	1	0	0	0
F5	1	1	1	1	0	1	1	0	0	0	0
F6	1	1	1	1	1	0	1	1	0	0	0

Table 10
The damage morphology of the differential capacitance-voltage converters

	Burned morphology of aluminum strip	Diode breakdown morphology
Faulty circuit sample 1		
Faulty circuit sample 2		
Faulty circuit sample 3		

Table 11The feature parameters function Table 2 of output saturation fault mode for fault circuit samples1-6.

	a1	a2	аЗ	b1	<i>b</i> 2	с	d1	d2	d3	d4	result
F1	1	1	1	1	1	1	1	1	0	0	0
F2	1	1	1	1	1	1	1	1	0	0	0
F3	1	1	1	1	1	1	1	1	0	0	0
F4	1	1	1	1	1	1	1	1	1	1	1
F5	1	1	1	1	0	1	1	0	0	0	0
F6	1	1	1	1	1	0	1	1	0	0	0

If F (a1, a2, a3, b1, b2, b3, c, d1, d2, d3, d4) = 1, the failure mode is the output saturation of the servo circuit caused by the disconnection of external lead bonding wire connecting the pin7, and if F (a1, a2, a3, b1, b2, b3, c, d1, d2, d3, d4) = 0, the failure mode is not this one. It is clear that the faulty sample 4 satisfies this feature parameter.

For fault sample 5, the feature parameters suitable for this fault mode are extracted. When performing the grades setting, b1 and b2 of the second-level decision feature parameters consisting of the self-test positive saturation output voltage (V_{sat1}) and self-test negative saturation output voltage (V_{sat2}) are changed. If the positive saturation output voltage of the self-test is 10-13 V, set b1 to 1, otherwise, set it to 0. If the negative saturation output voltage is still 10-13 V, set b2 to 1, otherwise, set b2 to 0. Meanwhile, set the loss angle tangent of the damping capacitor CAP8 to the third level of the characterization parameter from new, and set c to 1 if the loss angle tangent is greater than 0.001, otherwise set c to 0. At this point, the feature parameters of these faulty circuit samples are normalized, see Table 12.

From the above settings, the discriminant about the feature parameters of the output saturation failure mode caused by the internal breakdown and short circuit of damping capacitor CAP8 of its differential capacitance-voltage converter is obtained, which can be expressed as equation (3).

$$F(a1,a2,a3,b1,b2,b3,c) = (a1 \& a2 \& a3) \& (b1 \& b2 \& b3) \& (c)$$

$$(3)$$

If F(a1, a2, a3, b1, b2, b3, c) = 1, the failure modes is the output saturation of the servo circuit caused by the internal breakdown and short circuit of damping capacitor CAP8 of its differential capacitance-voltage converter, and if F(a1, a2, a3, b1, b2, b3, c) = 0, the failure mode is not this one. It is clear that the faulty sample 5 satisfy this feature parameter.

For fault sample 6, the feature parameters suitable for this fault mode are extracted. When performing the grades setting, the waveform and amplitude of the reference triangle wave generator as the third-level decision feature parameters is changed. If the reference triangle wave has no waveform, it is set to 1. If the waveform and amplitude of the reference triangle wave are normal, set it to 0. Meanwhile, set the bias resistor R2 of reference triangle wave generator to the fourth-level of the feature parameter and set d to 1 if the baias resistor R2 is open, otherwise set to 0. At this point, the feature parameters of these faulty circuit samples are normalized, see Table 13.

From the above settings, the discriminant about the feature parameters of the output saturation failure mode caused by open circuit of bias resistance R2 of its reference triangle wave generator is obtained, which can be expressed as equation (4).

$$F(a1,a2,a3,b1,b2,b3,c) = (a1 \& a2 \& a3) \& (b1 \& b2 \& b3) \& (c) \& (d)$$

$$\tag{4}$$

If F(a1, a2, a3, b1, b2, b3, c, d) = 1, the failure mode is the output saturation of the servo circuit caused by open circuit of bias resistance R2 of its reference triangle wave generator, and if F(a1, a2, a3, b1, b2, b3, c, d) = 0, the failure mode is not this one. It is clear

Table 12The feature parameters function Table 3 of output saturation fault mode for fault circuit samples1-6.

	a1	a2	аЗ	b1	<i>b</i> 2	c	result
F1	1	1	1	1	0	0	0
F2	1	1	1	1	0	0	0
F3	1	1	1	1	0	0	0
F4	1	1	1	1	0	0	0
F5	1	1	1	1	1	1	1
F6	1	1	1	1	0	0	0

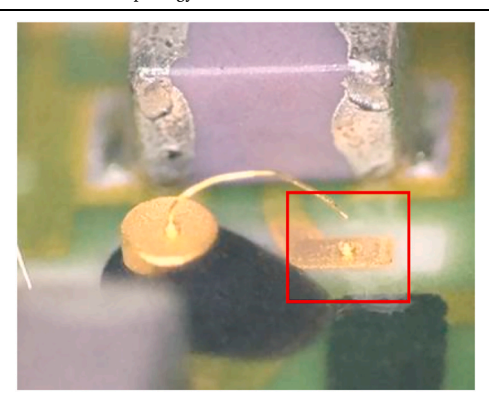
Table 13The feature parameters function Table 4 of output saturation fault mode for fault circuit samples1-6.

	a1	a2	a3	b1	<i>b2</i>	c	d	result
F1	1	1	1	1	1	0	0	0
F2	1	1	1	1	1	0	0	0
F3	1	1	1	1	1	0	0	0
F4	1	1	1	1	1	0	0	0
F5	1	1	1	1	0	0	0	0
F6	1	1	1	1	1	1	1	1

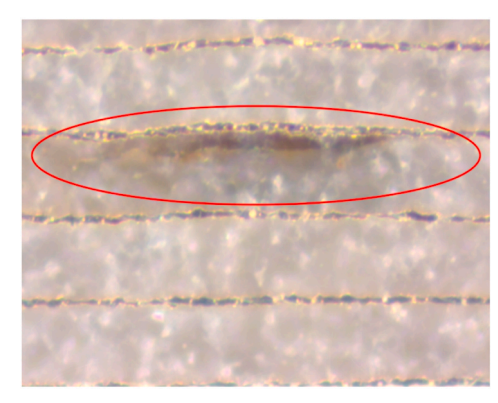
Table 14The failure morphology of the faulty circuit samples4-6.

Bonding wire disconnection morphology of faulty circuit sample 4

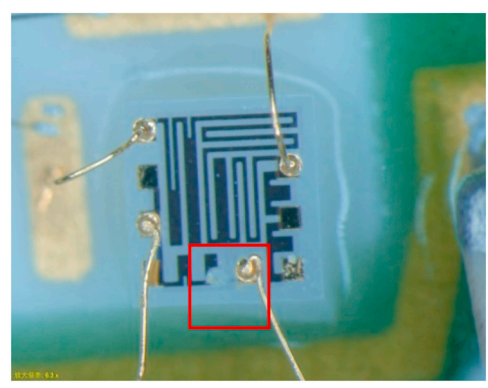




Breakdown morphology of failed capacitor of faulty circuit sample 5



Resistance corrosion morphology of faulty circuit sample 6



that the faulty sample 6 satisfies this feature parameter.

For the faulty circuit samples4-6, combined with the modular characteristics of hybrid integrated circuit, the feature parameters of corresponding fault modes are extracted, and the judgment of appropriate fault feature parameters are set. Using the fault diagnosis method mentioned in this paper, it is quickly and accurately found that the output saturation of the faulty circuit sample4 is caused by the disconnection of external lead bonding wire connecting the pin7, that of the faulty circuit sample5 is caused by the internal breakdown and short circuit of damping capacitor CAP8 of its differential capacitance-voltage converter, and that of the faulty circuit sample6 is caused by open circuit corrosion of bias resistance R2 of its reference triangle wave generator. The failure morphology is shown in Table 14.

4.2. Damage sample analysis

Although the substrate of the faulty circuit sample3 is mechanically damaged and cracked when the cap is opened, as shown in

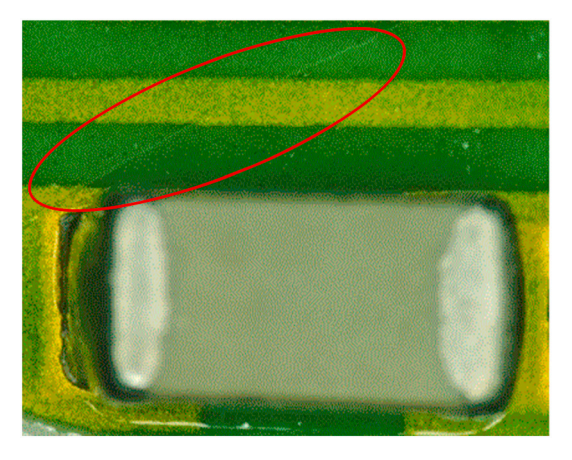


Fig. 9. Cracking morphology of substrate of the fault circuit sample 3.

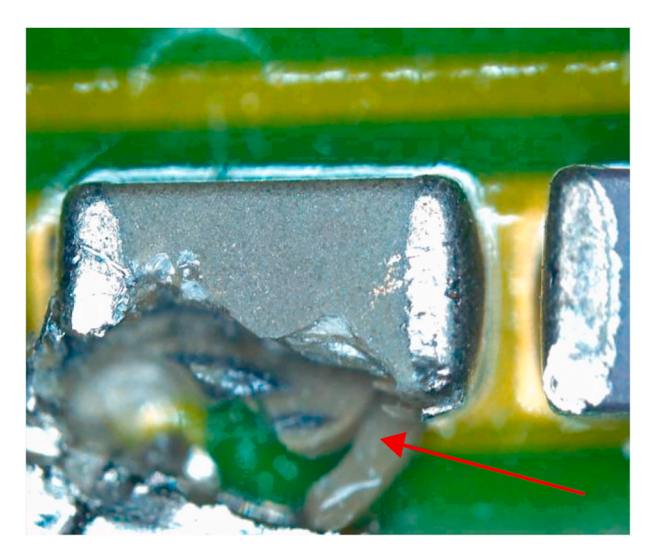


Fig. 10. Capacitance damage morphology of the faulty circuit sample 7.

Table 15The diode characteristic voltmeter of the faulty circuit sample 7.

	V_{T1}	V_{T2}
Faulty circuit sample 3	0.387	0.384
Qualified circuit	1.44	1.44

Fig. 9, it can be seen from the above analysis that the fault has been located, so the final analysis result has not been affected.

The output of the faulty circuit sample7 is saturated during the accelerometer test, but the sample is damaged when the system was separated, as shown in Fig. 10.

For this condition, the diode characteristic voltage from pin7 to pin8 and from pin8 to pin7 is directly tested with a digital voltmeter, and the characteristic curve between pin7 and pin8 is also tested. The test shows that the diode characteristic voltage is abnormal, as shown in Table 15 and the characteristic curve is abnormal, as shown in Fig. 11. It can be concluded that the fault is the output saturation of the circuit mentioned in the previous section.

When the cap is opened, it is found that the diode of differential capacitance detector of the faulty circuit sample7 is broken down. See Table 16 for the fault morphology. This failure mode is consistent with the failure prediction.

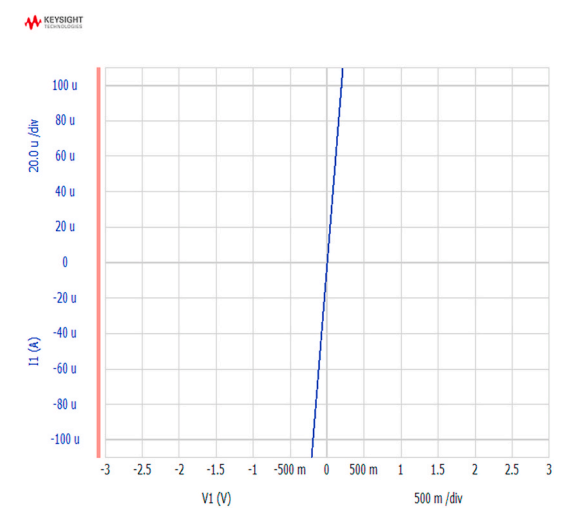
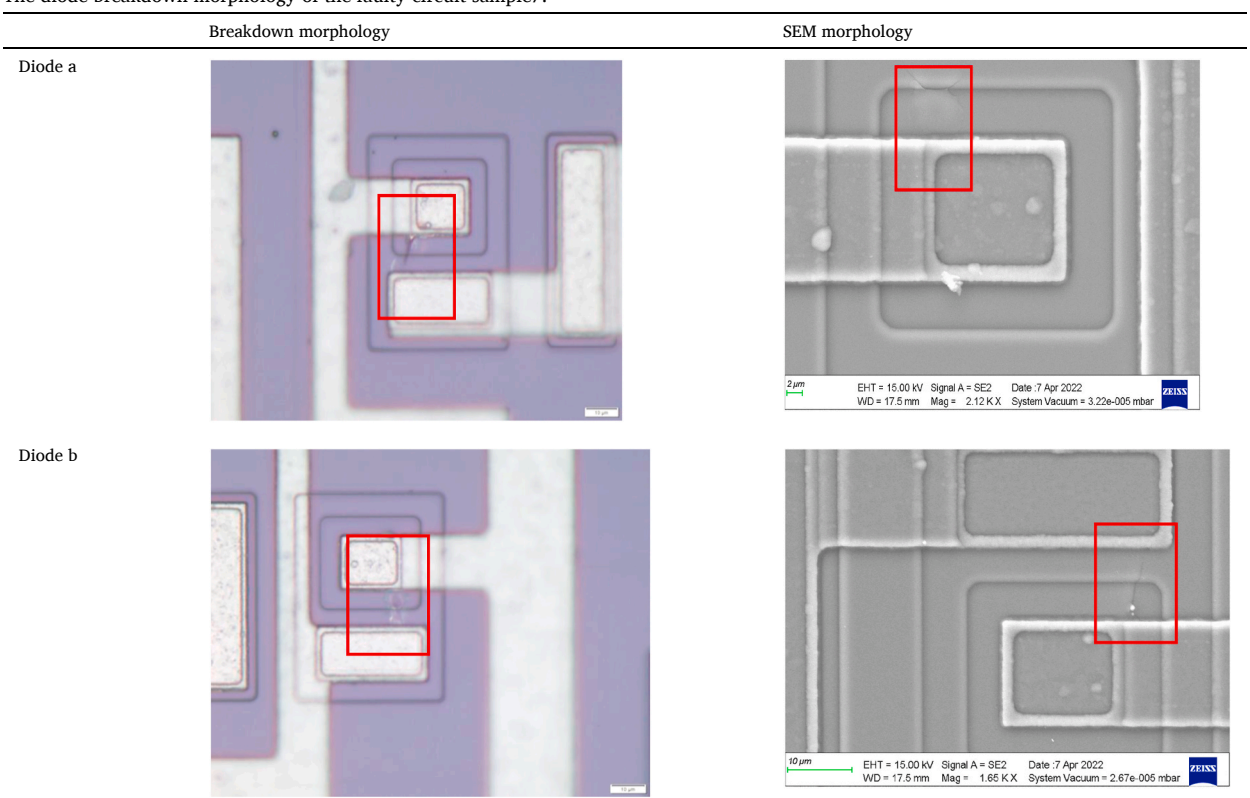


Fig. 11. The I-V characteristic curve between the pin7 and pin of the faulty circuit sample 7.

Table 16
The diode breakdown morphology of the faulty circuit sample7.



4.3. Discussion

It is more appropriate and perfect to analyze the intact samples by using the fault diagnosis method of feature parameters extraction, such as the faulty circuit samples1, 2, 4, 5, and 6. The analysis of damage samples can be divided into two categories. One is damaged after the cap is opened, but the feature electrical parameters have been extracted. The analysis of this type of cases using the fault diagnosis method of electrical parameters extraction is suitable, and the analysis results will not be affected, such as the faulty circuit sample3. The other is damaged before the cap is opened. It is difficult to analyze such cases, such as circuit the faulty sample7.

The reason is that the fault mode is easily affected by the damage when the accelerometer is separated, which may lead to the inability to extract complete or effective feature electrical parameters, so the complete feature parameter extraction method is not applicable to this situation. This situation needs to be analyzed by a more accurate feature parameter extraction method, but the precise feature parameters are limited by the measurability of the parameters, resulting in the limitations of this method.

Compared with the traditional fault analysis manner, the fault circuit analysis method proposed in this paper is over 30% more efficient, with 15% higher success rate and 100% fault analysis accuracy.

4.4. Improvement measures

For the different output saturation failure modes mentioned above, corresponding improvement measures are proposed.

- (1) In view of the output saturation of the accelerometer servo circuit caused by the electrical damage to the differential capacitance detector, such as the faulty circuit samples1, 2, 3, and 7, the insulated rubber tube can be used to prevent the introduction of abnormal electrical stress or ESD of mechanical mode at pin7 and pin8 when the accelerometer sensor is matched with the servo circuit. At the same time, a plug-in interconnection structure is designed. The structure achieves the electrical interconnection between the circuit and the sensor through the elastic cylindrical connector, which ensures that the pin7 and pin8 are no longer led out in the form of the ports. And the circuit with this structure can eliminate this fault mode completely [9].
- (2) For the output saturation of the circuit caused by the disconnection of the gold bonding wire connecting pin7, like the faulty circuit sample 4, it is found that its AOI and energy spectrum of gold bonding wire disconnection section are normal, and it is obvious that the fault is caused by the abnormal mechanical stress of the bonding wire from the analysis of the broken morphology. It is necessary to avoid misoperation and strengthen the protection of the circuit during the packaging process.
- (3) The output saturation of the circuit caused by the internal breakdown and short circuit of damping capacitor of its differential capacitance-voltage converter is a fault that is difficult to detect, such as the faulty circuit samples 5. For this fault, the loss angle tangent test, ultrasonic scanning test and voltage withstand test shall be carried out on the multilayer ceramic dielectric capacitor before the circuit assembly, and the multilayer ceramic dielectric capacitor with a thickness of more than 1 mm and a thicker dielectric layer shall be used.
- (4) The output saturation of the circuit caused by open circuit due to bias resistance corrosion of reference triangle wave generator involves the storage environment and manufacturing process, such as the faulty circuit samples 6. The circuit is a non-airtight package and is not suitable for long-term storage in a humid environment. Therefore, the manufacturing process is improved, that is, the amount of adhesive applied to the cover plate is controlled during packaging process, so that the adhesive forms a continuous coating layer on the bonding surface of the cover plate. Besides, the self-inspection and patching of the circuit are conducted before curing to ensure that the cover plate is coated with adhesive continuously and without pores. Furthermore, in order to fundamentally solve the problem fundamentally, a hermetically sealed accelerometer servo circuit is designed.

5. Conclusion

All in all, the fault analysis of hybrid integrated circuits is a complex project. The electrical parameters of the accelerometer servo circuit are set on the basis of meeting the application requirements, but these parameters are often not enough for accurate fault diagnosis, and the fault mode cannot be characterized by them effectively and accurately during fault detection. Compared with the traditional fault analysis method which has full coverage of critical fault node parameters when necessary, the fault detection and analysis method based on the feature electrical parameters extraction only needs to extract the parameter groups that characterize the fault features. At the same time, compared with the physical analysis method, this method not only effectively utilizes the electrical characteristics of the hybrid integrated circuit, but also does not need to rely too much on the integrity of the circuit and numerous instruments. What's further, the method has a higher success rate, and improves the reliability of failure analysis. That is to say, the physical characterization analysis has become a verification method. In a word, the new analysis method covers the logic analysis of circuit modularity and the correspondence analysis between physical representation and the circuit feature parameters. This method has higher efficiency compared to traditional fault dictionary methods, and has strong targeting and high analytical reliability compared to the large amount of data required based on machine learning models. It has good applicability in the field of electronics. According to the feedback data statistics, the output saturation faults accounts for 59.6% of the total number of failed circuits in the use process, and the faults caused by the electrical damage to differential capacitance detector is 78.26% of the total number of circuits with saturation output. It can 100% detect the output saturation fault of the accelerometer servo circuit caused by the electrical damage to the differential capacitance detector and the vast majority of other causes. Besides, the method can also be well applied to the fault location and analysis of accelerometer servo circuits and other hybrid integrated circuits. It is of great significance to promote the fault analysis level of hybrid integrated circuits.

Data availability statement

The data supporting this study are included in the article.

Ethics declarations

This is the author's original work and has not been published previously. No ethical issues were related to this study.

CRediT authorship contribution statement

Ming Zhang: Writing – review & editing, Writing – original draft, Validation, Methodology, Conceptualization. Xin Xu: Visualization, Formal analysis. Likun Xu: Investigation. Xiaoming Ruan: Data curation. Duan Zhou: Validation. Zhenshan He: Supervision, Investigation.

Declaration of competing interest

The authors declare that they have no known competing financial interests or personal relationships that could have appeared to influence the work reported in this paper.

References

- [1] S.A. Foote, D.B. Grindeland, Model QA3000 Q-Flex accelerometer high performance test results, IEEE Aero. Electron. Syst. Mag. 7 (6) (1992) 59-67.
- [2] B. Hathi, A.J. Ball, G. Colombatti, et al., Huygens HASI servo accelerometer: a review and lessons learned, Planet. Space Sci. 57 (12) (2009) 1321–1333.
- [3] J. Shieh, J.E. Huber, N.A. Fleck, et al., The selection of sensors, Prog. Mater. Sci. 46 (3) (2001) 461-504.
- [4] M. Vellekoop, B. Jakoby, R. Chabicovsky, Development trends in the field of sensors, e & i Elektrotechnik and Informationstechnik 120 (11) (2003) 388–394.
- [5] G. Yu, J. Wang, W. Wang, Research and application of inclinometer based on servo-accelerator of quartz flexibility, in: 8th International Conference on Electronic Measurement and Instruments, ICEMI. Xian. Inst. Of Elec. and Elec. Eng. Computer Society, vol. 2007, 2007, pp. 4256–4260.
- [6] M. Zhang, H.H. Wan, X. Xu, X.M. Ruan, Servo circuit of quartz flexible accelerometer with low power consumption and high integration, Guangzhou, in: SPIE International Conference on Optoelectronic Materials and Device, 2020, p. 11767001, 11767001.
- [7] R. Cao, Y. Chen, R. Kang, Failure mechanism analysis of quartz accelerometer under vibration condition. Prognostics and System Health Management Conference, IEEE, 2011, pp. 1–5.
- [8] H.H. Wan, X. Xu, M. Zhang, et al., Research on the function failure of accelerometer servo circuit caused by hydrolysis and corrosion, Eng. Fail. Anal. 131 (2022) 105828.
- [9] M. Zhang, X. Xu, H.H. Wan, et al., Failure analysis of accelerometer servo circuit caused by electrical damage to differential capacitance detector, J. Fail. Anal. Prev. 22 (2022) 926–933
- [10] Y. Rao, B.L. Xu, T. Jing, et al., Research on fault tree comprehensive analysis method based on TOPSIS, Microelectron. Comput. 34 (2017) 28-33.
- [11] D. Binu, B.S. Kariyappa, A survey on fault diagnosis of analog circuits: taxonomy and state of the art, AEU International Journal of Electronics and Communications 73 (2017) 68–83.
- [12] D.X. Sun, Y.Y. Yang, H.C. Wang, etc. Multi-state dynamic fault tree analysis method for avionics computing platform, Microelectron. Comput. 34 (2017) 12–16, 20.
- [13] F. Li, P.Y. Wo, Fault detection method for the subcircuits of a cascade linear circuit, IEEE Transactions on Circuits and Systems I: Fundamental Theory and Applications 47 (2002) 1245–1258.
- [14] C.K. Ho, P.R. Shepherd, F. Eberhardt, et al., Hierarchical fault diagnosis of analog integrated circuits, IEEE Transactions on Circuits and Systems I Fundamental Theory and Applications 48 (2000) 921–929.
- [15] W. Toczek, R. Zielonko, A. Adamczyk, A method for fault diagnosis of nonlinear electronic circuits, Measurement 24 (1998) 79-86.
- [16] M. Catelani, S. Giraldi, A measurement system for fault detection and fault isolation of analog circuits, Measurement 25 (1992) 115-122.
- [17] J.A. Starzyk, L. Don, Z.H. Liu, et al., Entropy-based optimum test points selection for analog fault dictionary techniques, IEEE Trans. Instrum. Meas. 53 (2004) 754–761.
- [18] H. Ke, H. Stratigopoulos, S. Mir, Fault diagnosis of analog circuits based on machine learning. IEEE Design, Automation & Test in Europe Conference & Exhibition, 2010, pp. 1761–1766.
- [19] Y. He, Y. Tan, Y. Sun, Class-based neural network method for fault location of large-scale analogue circuits, IEEE International Symposium on Circuits & Systems (2003) 733–736.
- [20] F. Aminian, M. Aminian, H.W. Collins, Analog fault diagnosis of actual circuits using neural networks, IEEE Trans. Instrum. Meas. 51 (2002) 544-550.
- [21] W. He, Y. He, B. Li, C. Zhang, A naive-bayes-based fault diagnosis approach for analog circuit by using image-oriented feature extraction and selection technique, IEEE Access 8 (2020) 5065–5079, https://doi.org/10.1109/ACCESS.2018.2888950.
- [22] C. Zhang, Y. He, L. Yuan, S. Xiang, Analog circuit incipient fault diagnosis method using DBN based features extraction, IEEE Access 6 (2018) 23053–23064, https://doi.org/10.1109/ACCESS.2018.2823765.
- [23] C. Zhang, Y. He, B. Du, et al. Transformer Fault diagnosis method using IoT based monitoring system and ensemble machine learning [J]. Future Generat. Comput. Syst. doi: 10.1016/j.future.2020.03.008..
- [24] Xiaosong Hu, Kai Zhang, Kailong Liu, Xianke Lin, Satadru Dey, Simona Onori, Advanced Fault diagnosis for lithium-ion battery systems, TechRxiv. Preprint (2020). https://doi.org/10.36227/techrxiv.11777448.
- [25] Z. Liu, Q. Ahmed, J. Zhang, G. Rizzoni, H. He, Structural analysis based sensors fault detection and isolation of cylindrical lithium-ion batteries in automotive applications, Control Eng. Pract. 52 (Jul. 2016) 46–58.
- [26] E. Balaban, A. Saxena, P. Bansal, K.F. Goebel, S. Curran, Modeling, detection, and disambiguation of sensor faults for aerospace applications, IEEE Sensor. J. 9 (12) (Dec. 2009) 1907–1917, https://doi.org/10.1109/JSEN.2009.2030284.
- [27] S. Simani, C. Fantuzzi, S. Beghelli, Diagnosis techniques for sensor faults of industrial processes, IEEE Trans. Control Syst. Technol. 8 (5) (Sept. 2000) 848–855, https://doi.org/10.1109/87.865858.
- [28] E. Kiyak, Ö. Çetin, A. Kahvecioğlu, Aircraft sensor fault detection based on unknown input observers, Aircraft Eng. Aero. Technol. 80 (5) (2008) 545-548.
- [29] R. Xiong, Q. Yu, W. Shen, C. Lin, F. Sun, A sensor fault diagnosis method for a lithium-ion battery pack in electric vehicles, IEEE Trans. Power Electron. 34 (10) (Oct. 2019) 9709–9718. https://doi.org/10.1109/TPEL.2019.2893622.